THE ASTROPHYSICAL JOURNAL, 424:1005–1013, 1994 April 1

GRAVITATIONAL TIDES ON JUPITER. III. ATMOSPHERIC RESPONSE AND MEAN FLOW ACCELERATION

PETROS J. IOANNOU AND RICHARD S. LINDZEN
Center for Meteorology and Physical Oceanography, Massachusetts Institute of Technology, Cambridge, MA 02139
Received 1993 April 5; accepted 1993 October 8

ABSTRACT

The gravitational tidal response at the visible cloud level of Jupiter is obtained as a function of static stability in the planetary interior. It is suggested that confirmation of the presence of static stability in the planetary interior could be achieved by observing tidal fields at cloud level. We also calculate the mean flow accelerations induced by tidal fields and suggest that, if the interior is even marginally statically stable, the tides may provide the momentum source maintaining the alternating zonal jets observed at the cloud level of the planet.

Subject heading: planets and satellites: individual (Jupiter)

1. INTRODUCTION

The theory of the gravitational tidal excitation of the Jovian planets was presented in previous papers (Ioannou & Lindzen 1993a, b, hereafter, respectively, ILa and ILb) where we have shown that the tidal response depends crucially on the static stability in the interior of the planet. The common assumption is that the interior is neutrally buoyant. Although such an assumption adequately describes the mean thermodynamic structure of the interior, it filters all internal gravity waves, allowing only acoustic propagation, with major implications for the tidal response. In the absence of static stability in the interior, a neutrally buoyant material surface deforms to become nearly an equilibrium equipotential surface. However, the dynamic tidal response is proportional to the difference of the displacement of the material surface from that due to the equilibrium tide. Consequently, unless the interior has some stability, the tidal response will be insignificant even though the tidal potential at the surface of the planet may be large (i.e., the tidal potential at the surface of Jupiter due to Io is roughly two orders of magnitude stronger than that of the Moon on Earth).

Fortunately, it turns out that we can plausibly constrain the stability of the interior of the Jovian planets by consideration of the tidal dissipation required by orbital evolution of the planet's satellites. For example, if Io originated at the surface of Jupiter and moved to its present location in 4.5 billion years, its orbital energy increased by 10^{32} J which requires a tidally induced dissipation of the order of 10^{15} W. The estimated tidal dissipation factor Q, defined as the ratio of the maximum tidal energy to that lost per cycle, is thus estimated to be of the order $Q \approx 10^4$–10^5. An estimate of the energy lost per cycle can be provided by the tidal energy radiated from the planet (Houben 1978). It should be noted that radiating waves must ultimately be dissipated at sufficiently great heights either by wave breaking or eventually by molecular diffusion. This is the type of dissipation we are generally referring to, and is to be distinguished from wave dissipation at lower levels which can even inhibit the wave amplitudes required. In ILb we calculated this energy dissipation and the corresponding Q as a function of the static stability in the interior which for a polytrope of index 1 is proportional to $\Gamma_1 - 2$, where Γ_1 is the compressibility at constant entropy. The results of such a calculation are presented in Figure 1. Note that a neutrally buoyant interior ($\Gamma_1 = 2$) gives dissipation which is too small to account for the evolution of the orbit of Io. However, introduction of some static stability in the interior produces wave fluxes which are consistent with orbital evolution. The peaks in the response curve reflect the complex response properties of the interior waveguide. Note that the radiated flux exhibits great sensitivity to the interior static stability, leading to a radiated wave flux which can reach the observed theral emission of Jupiter (9×10^{17} W).

Encouraged by the agreement with the evolutionary theory of the orbit of Io we will, in this paper, investigate further implications of the existence of nonvanishing static stability in the interior of the planet.

2. TIDAL FIELDS AT THE ATMOSPHERIC ENVELOPE OF JUPITER

The expansion of the perturbing tidal potential at the surface of Jupiter due to Io in terms of Hough functions provides the measure of excitation of the various meridional modes and is given in units of $m^2 s^{-2}$ by

$$\begin{aligned}\Omega = &-275.6\Theta_2 - 77.2\Theta_4 - 39.1\Theta_6 - 24.7\Theta_8 \\ &- 17.3\Theta_{10} - \cdots - 5.9\Theta_{20} - \cdots \\ &- 104.92\Theta_{-2} - 41.51\Theta_{-4} - \cdots ,\end{aligned} \tag{2.1}$$

where $\Theta_n \equiv \Theta_n^{\sigma,s}(\theta)$ are the appropriate Hough functions with, $\sigma = 2.7 \times 10^{-4}$ s^{-1} the frequency of the forcing (the corresponding period is 6.47 hr), $s = 2$ the zonal wavenumber and, θ the colatitude (tabulations of the Hough functions and further details can be found in ILa). If the planet were a passive medium the tidal response would be concentrated in the gravest meridional mode, which is approximately proportional to the associated Legendre polynomial $P_2^2(\theta)$, and the relative magnitude of the higher modes would be in proportion to the coefficients of eq. (2.1) (refer to Fig. 2).

Selective amplification of specific meridional modes in a stratified atmosphere occurs in regions where that mode is radially propagating. The condition for radial propagation is given in its simplest form for the case of an ideal gas atmosphere for which the hydrostatic approximation is accurate ($N \gg \sigma$, where N is the Brunt-Väisälä frequency). In such circumstances the index of refraction is simply

$$m^2 = \frac{N^2 H^2}{g h_n} - \frac{1}{4}, \tag{2.2}$$

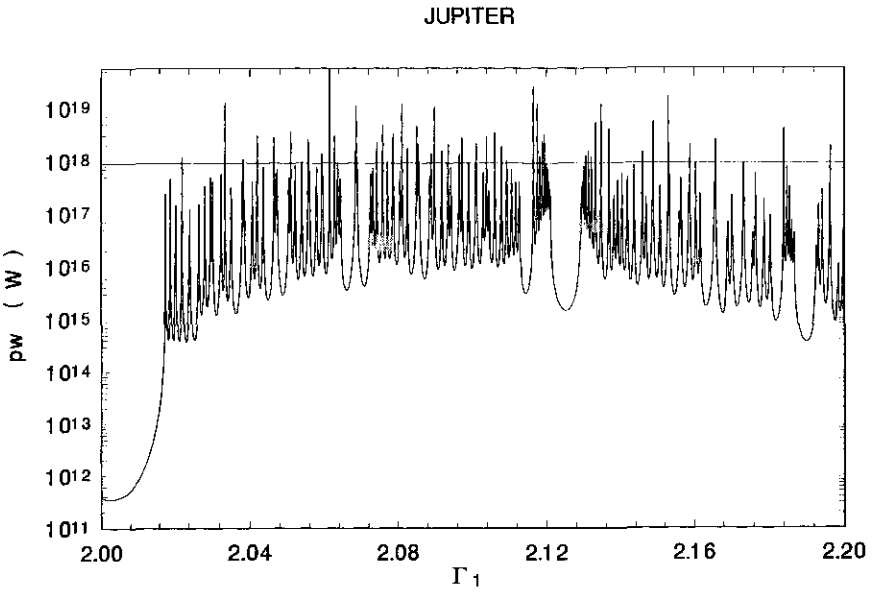

FIG. 1.—Total energy flux $\overline{pw}$ in Watts, integrated over the surface of Jupiter, as a function of Γ_1. A statically neutral interior corresponds to $\Gamma_1 = 2$. The straight line indicates the observed emitted power.

where H is the local scale height, g the acceleration due to gravity, and h_n the equivalent height associated with the nth Hough mode, Θ_n (for the values of the equivalent heights refer to ILa). Generalization of equation (2.2) for polytropic self-gravitating and nonhydrostatic planetary interiors can be found in ILb. As first noted by Lindzen (1991), equation (2.2) implies that for the same thermodynamic structure the higher Hough modes are favored for propagation. Also for a given Hough mode, an increase of mean temperature in inverse proportion to the local Brunt-Väisälä frequency does not alter the index of refraction. The Hough modes that radially propagate, amplify as $e^{x/2}$, where x is the radial distance measured in units of the scale-height, in order to maintain constancy of energy density in the exponentially stratified medium. Consequently, the radial structure equation provides a high pass filter for the lower order meridional modes. In what follows, we will concentrate on modes with positive equivalent depth. The modes of negative equivalent depth are important only for latitudes poleward of the critical latitude, $\phi_{cr} \approx 50°$, and they are radially evanescent in the presence of stratification.

In an idealized treatment of the planet there are two regions in which propagation can occur: the stably stratified ideal gas atmospheric envelope and regions in the polytropic interior that possess adequate static stability. It turns out (as shown in ILb) that the region of propagation in the interior of the planet forms a waveguide bounded below, well within the planet, by the radius at which $N = \sigma$, and above, in the ideal gas atmosphere, below the cloud cover, where the temperature is not great enough to support propagation. Peak tidal response in the atmosphere occurs when the phase integral in the interior waveguide is equal to $(n + 1/2)\,\pi$, with n integer, which will be referred in the following as the quantization condition.

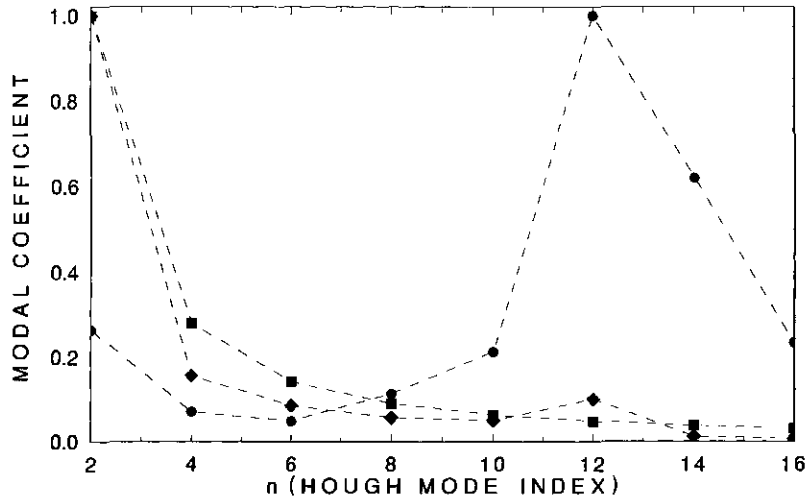

FIG. 2.—The tidal temperature response at cloud level is decomposed in terms of Hough functions and the normalized coefficient of each mode is indicated. The squares are the normalized coefficients of the tidal potential. The diamonds show the coefficients of the response when the interior is neutral. The circles are the normalized coefficients of the response for a stable interior with $\Gamma_1 = 2.05$.

It may seem surprising that the maximal wave energy flux in the atmosphere is attained when the inner waveguide satisfies the quantization condition; however, this is the norm for leaky waveguides. This property of leaky waveguides is best elucidated with a two-layer example adapted from Gill (1982, p. 148; an example of a related phenomenon in the Venusian atmosphere was examined by Hou & Farrell [1987]). Consider internal gravity waves excited at $z = 0$ by imposing a vertical velocity, w, at $z = 0$:

$$w = A \exp(ikx + im_i z - i\omega t), \tag{2.3}$$

with horizontal wavenumber k, vertical wavenumber m_i, and frequency ω. Assume that the Brunt-Väisälä frequency is $N_1 < z < H$ and $N_2 > N_1$ in $z > H$. For simplicity we assume parameters for which the waves propagate in the whole domain. Then $m_1 < m_2$ [from the dispersion relation $m_i^2 = k^2(N_i^2 - \omega^2)/\omega^2$] and the vertical energy flux is given by

$$F \sim \frac{\omega m_2 A^2}{k^2} \frac{1}{1 + (m_2^2/m_1^2 - 1)\sin^2 m_1 H}. \tag{2.4}$$

For $m_1 < m_2$ the maxima in the wave flux response occur when the lower waveguide is exactly tuned, i.e., when $m_1 H = n\pi$. Furthermore the peak flux relaxes to a small value ($\sim m_1^2/m_2^2$ of the maximum) with a half-width of $\sim 1/m_2$. The leaky duct allows quasi-resonant amplification which allows the leaking wave amplitudes to increase.

In our case the size of the interior waveguide is proportional to $\Gamma_1 - 2$ and it is larger for the higher modes. However, the size of the wave guide, measured in scale heights, does not increase linearly with the interior stratification. Although there are ~ 18 scale heights between the visible cloud level and the center of the planet, only 4 scale heights are between 0.9 of the radius of the planet and the center. As a result, an increase in Γ_1 leads only to a marginal increase in the size of the interior waveguide, and the tidal response rapidly approaches an asymptotic limit (cf. Fig. 1 disregarding the peaks which are due to selective tuning of the interior waveguide). The selective amplification of the modes can be quantified by expanding the meridional dependence of the tidal response in the atmosphere in terms of Hough modes, and plotting the coefficients of this expansion as a function of the mode index. This is done for the amplitude of the tidal temperature perturbation at the visible cloud level of the planet and shown in Figure 2. For a neutral interior the response at the cloud level is concentrated in the first meridional mode and the modal amplitudes are to a good approximation in the same ratio as the coefficients of the excitation given in equation (2.1) (the small relative amplification of the 12th mode is due to amplification in the atmospheric envelope below the cloud level). The presence of interior stratification leads to relative reinforcement of higher order modes. The specific mode that is reinforced depends on the tuning of the interior wave guide and could only be determined if the detailed structure of the stratification in the interior of the planet were known. It should be added that the shorter radial wavelengths associated with the higher modes satisfy the requirement for the quantization condition at smaller values of interior stratification. For example for the Θ_2 mode the quantization condition is first satisfied for $\Gamma_1 \approx 2.1$, for the Θ_6 mode for $\Gamma_1 \approx 2.084$, for the Θ_8 mode for $\Gamma_1 \approx 2.067$, for the Θ_{10} mode for $\Gamma_1 \approx 2.056$.

In the ideal gas atmospheric envelope, propagation again favors the higher order modes. The index of refraction for some higher order modes is plotted in Figure 3 for different vertical structures of the static stability. The visible cloud height (≈ 150 mbar) is located 1 scale height below the reference level in this graph. The temperature structure in the atmosphere is shown in Figure 4. Observations extend down to approximately a level 2.5 scale heights below the reference level (refer to Lindal et al. 1981). The temperature high in the atmosphere, above the clouds, asymptotes to 155 K, and the curves shown in Figure 4 correspond to different values of the static stability in the deep atmosphere. The static stability below the reference level is exponentially relaxed to a lower constant value with an e-folding distance of 1 scale height. The dotted curve shows the temperature structure for the case in which the stability is relaxed to neutrality; the dashed curve corresponds to a Brunt-Väisälä frequency in the deep atmosphere which is 1/10 of the Brunt-Väisälä frequency at the reference level, $N_r \approx 75\ \sigma$; and the continuous curve corresponds to a deep atmospheric Brunt-Väisälä frequency which is one-fifth that at the reference level. The variation of the index of refraction in Figure 3 is

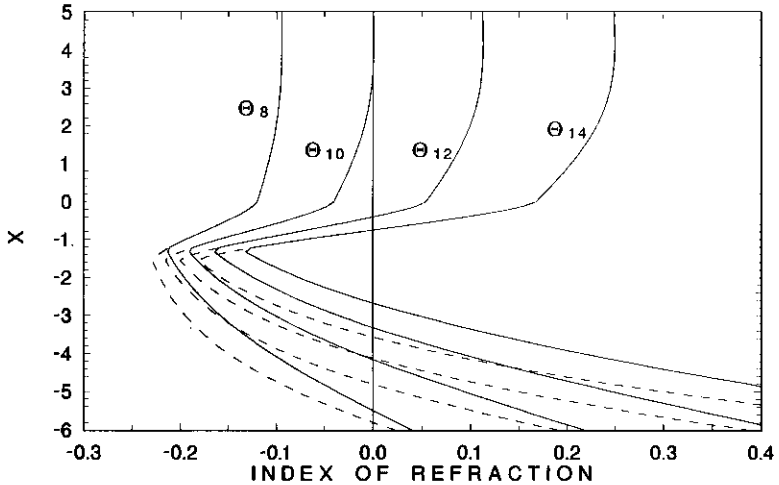

FIG. 3.—The index of refraction as a function of height measured in pressure scale heights for the meridional modes of order 8, 10, 12, 14. The reference level $X = 0$ corresponds to the Jovian tropopause. The transition to the polytropic interior has been placed at $X = -7$. The solid curve corresponds to a static stability which has a constant value $N = N_{trop}/10$, where N_{trop} is the tropopause Brunt-Väisälä frequency. The dashed curve corresponds to $N = N_{trop}/5$.

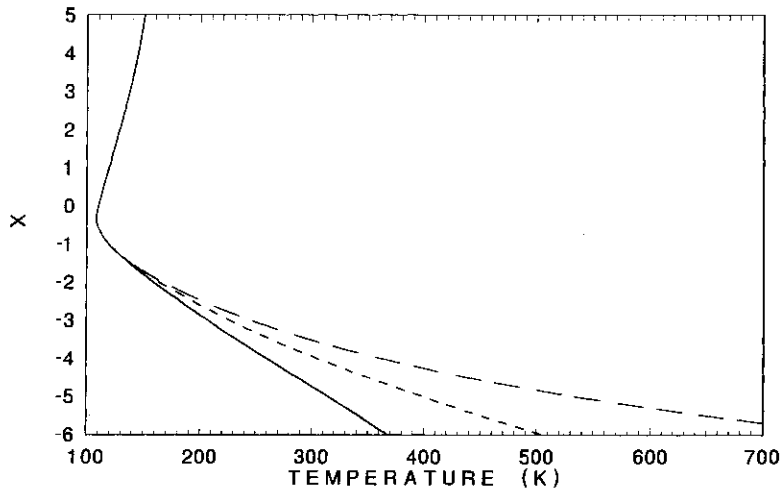

FIG. 4.—The mean temperature structure as a function of height measured in pressure scale heights. The temperature asymptotes in the stratosphere to 155 K. The three curves are for different static stabilities under the visible clouds which are located approximately at $X = -1$. The long-dashed curve assumes that the stability becomes neutral for $X < -1$, the short-dashed curve assumes that the Brunt-Väisälä frequency asymptotes to a value which is 1/10 of that at the tropopause, the continuous curve assumes that the Brunt-Väisälä frequency asymptotes to a value which is 1/5 of that at the tropopause. Observational values of the mean structure extend to $\sim X = -2$.

shown only for the latter two atmospheric structures. Above the clouds, propagation is possible for modes of order higher than the 10th; in the visible cloud region, reduction of the stability leads to trapping; and in the deeper atmosphere, propagation is again possible due to the higher temperature. Transition to the polytropic interior is usually placed 6–7 scale heights below the reference level. Consequently, if the polytropic interior is taken to be neutral, propagation below the cloud cover cannot provide the magnification requisite for a tidal response which is dominated by higher order modes at cloud level. In contrast, the presence of stratification in the interior leads to a tidal response at the cloud level which is, indeed, concentrated in the higher Hough modes. We have argued that producing the tidal dissipation necessary for orbital evolution, requires the presence of stratification in the interior of the planet. We have seen that this, in turn, implies that the tidal response at cloud level should be dominated by the higher Hough modes. This could provide observational confirmation of the existence of stability in the interior if such a tidal response were to be observed. It seems that temperature fluctuations of an amplitude as low as 0.07 K can be observed with Earth-based infrared telescopy (cf. Deming et al. 1989). For comparison we plot the maximum temperature response at cloud level as a function of Γ_1 in Figure 5. We note that the tidal temperature signal should be observable if the interior is adequately stratified.

Before presenting specific examples of the tidal response at cloud level, we comment on the physical relevance of the higher Hough modes and their tuning in the interior wave guide. In principle, the tuning of the interior wave guide and the slow convergence of the coefficients of the expansion of the excitation given in equation (2.1) could result, for special values of Γ_1, in tidal response dominated by a very high order Hough mode. However, this is unlikely to occur in practice. In the

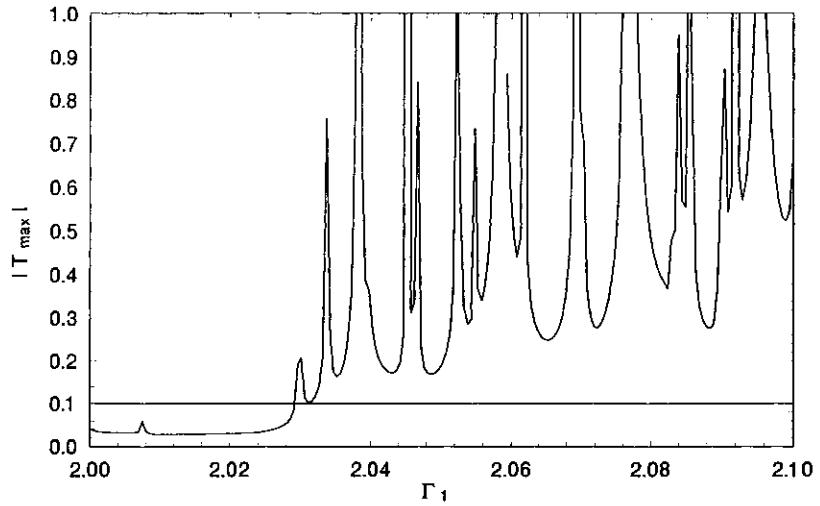

FIG. 5.—The magnitude of the equatorial tidal temperature response in K at cloud level as a function of the stability in the interior measured by Γ_1. The solid curve corresponds to 0.1 K; the observational resolution according to Deming et al. (1989) is 0.07 K.

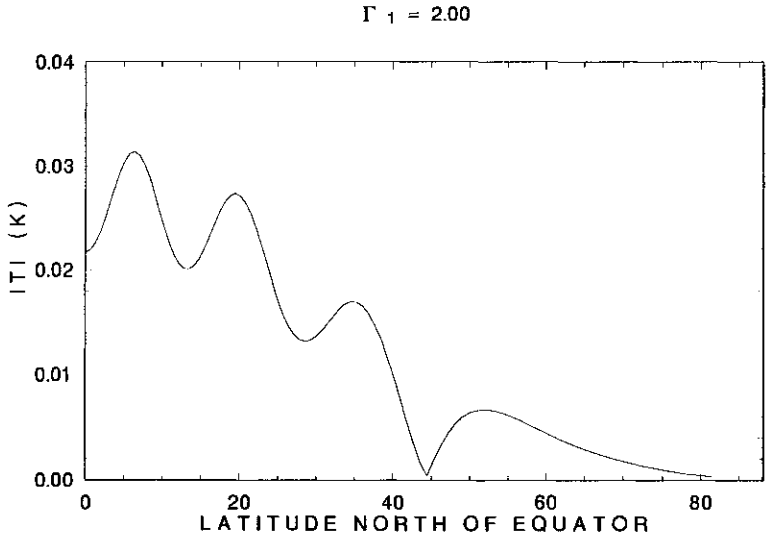

FIG. 6.—The latitudinal structure of the magnitude of the tidal temperature oscillation at cloud level for a neutral interior

terrestrial context it was demonstrated by Lindzen & Hong (1974) that inclusion of latitudinal variations in the mean temperature and wind fields effectively eliminates the coherent interference needed to tune the associated waveguides. The lateral homogeneity of the Jovian atmosphere, and the smaller horizontal scale (relative to the planetary radius) of the relevant modes, significantly reduces the severity of this constraint on Jupiter except for the high-order modes.

The tidal temperature is plotted for a neutral interior and for a stratified interior in Figures 6 and 7. The response, as already discussed, is, in the former case, concentrated in the gravest mode, while in the second case in a higher mode, which for the specific choice $\Gamma_1 = 2.05$ happened to be the 12th mode.

The vertical structure of the temperature field is shown in Figure 8. It is expected that the tidal fields cannot exceed an amplitude for which the lapse rate due to the total fields (the sum of the mean state and the tidal perturbation) becomes superadiabatic. When this occurs, secondary convective instabilities are expected to occur associated with breaking of the waves (Lindzen 1981). Above the breaking level, the tidal fields are expected to reach a saturated amplitude (Lindzen 1988). We can readily estimate the threshold amplitude for breaking, which, for the 10th and 12th modes on Jupiter, is associated with temperature fluctuations of the order of 60 K and corresponding vertical velocities of 6 ms^{-1}. As can be seen from Figure 5 at cloud level the tidal fields are unlikely to reach breaking amplitude. The breaking level for the example presented is expected to occur ~ 12 scale heights (i.e., ≈ 250 km) above the visible clouds.

The latitudinal structure of the tidal zonal velocity is shown in Figure 9, and its vertical structure is plotted in Figure 10 for $\Gamma_1 = 2.05$. Note that at the breaking level the zonal velocity is ≈ 50 ms^{-1}. The corresponding vertical velocity structure is shown in Figure 11.

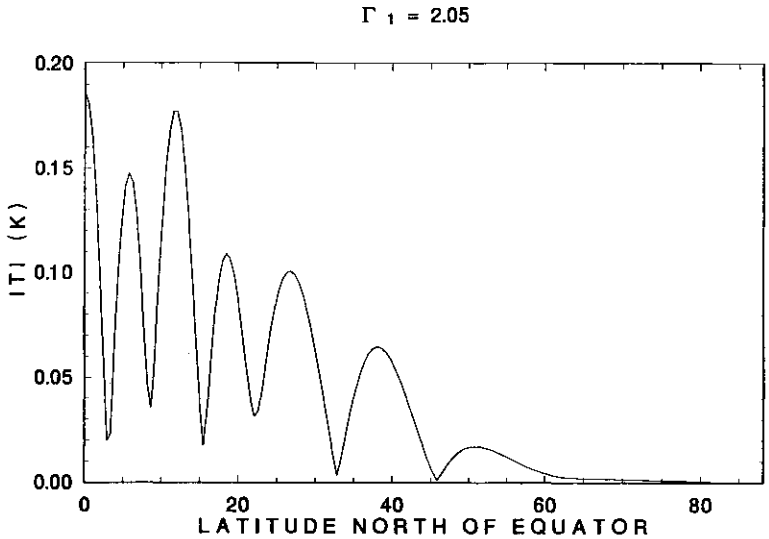

FIG. 7.—The latitudinal structure of the magnitude of the tidal temperature oscillation at cloud level for an interior with $\Gamma_1 = 2.05$. The dominant response is concentrated at the 12th mode (viz. Fig. 2).

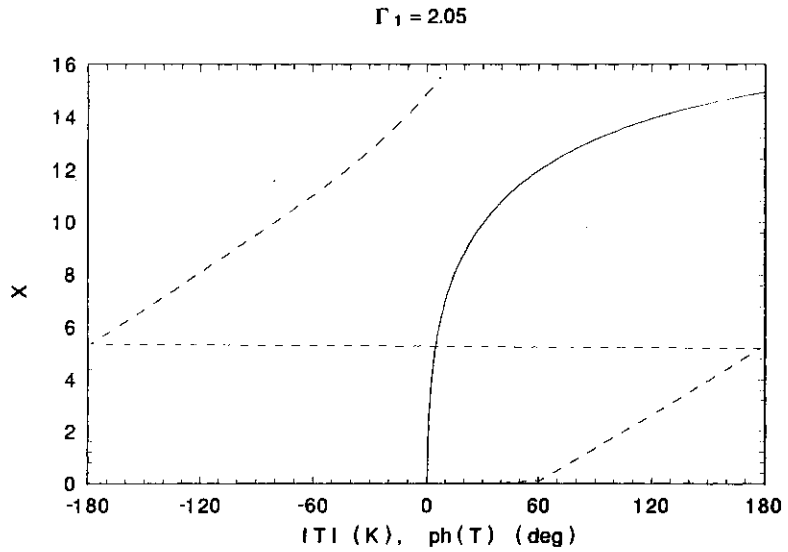

FIG. 8.—The vertical structure of the tidal temperature oscillation at the equator as a function of height, measured in pressure scale heights. In the interior $\Gamma_1 = 2.05$. The reference level $X = 0$ corresponds to the tropopause. The solid curve is the magnitude, the dashed curve is the phase in degrees. Breaking occurs at $X \approx 12$.

3. MEAN FLOW MODIFICATIONS INDUCED BY THE TIDAL FIELDS

To estimate the acceleration of the zonal mean flow by the tides, we zonally average the fully nonlinear zonal momentum equation, separating the fields into zonally averaged fields (denoted with a bar) and tidal eddy components to obtain:

$$[\rho_o \bar{v}]_t + 2\omega \cos\theta \overline{\rho u} = -\frac{1}{a \sin^2\theta}[\rho_o \overline{uv} \sin^2\theta]_\theta - [\rho_o \overline{vw}]_z , \tag{3.1}$$

where ω represents the angular velocity of the planet, a its radius, θ the colatitude, and z the vertical distance. Time and the spatial derivatives are denoted with a corresponding subscript. The fields pertaining to the initially motionless background mean state are denoted with the subscript o, so that ρ_o is the background density. The tidal fields are u, the southward meridional velocity; v the eastward zonal velocity; w the vertical velocity; p the tidal pressure; ρ the tidal density.

The tidal fields will force an Eulerian meridional circulation which will cancel, in the absence of transience, forcing, and dissipation, the pointwise acceleration induced by the tidal momentum divergence on the right-hand side of equation (3.1). Andrews & McIntyre (1976) and Boyd (1976) proved that this canceling meridional circulation will have stream function:

$$\bar{\psi} = \rho_o \frac{\overline{uT^p}}{T^p_{oz}} , \tag{3.2}$$

where

$$T^p = \ln\left[\frac{p}{p_r}\left(\frac{\rho}{\rho_r}\right)^{-\gamma}\right], \tag{3.3}$$

is the perturbation potential temperature, p_r and ρ_r are refer-

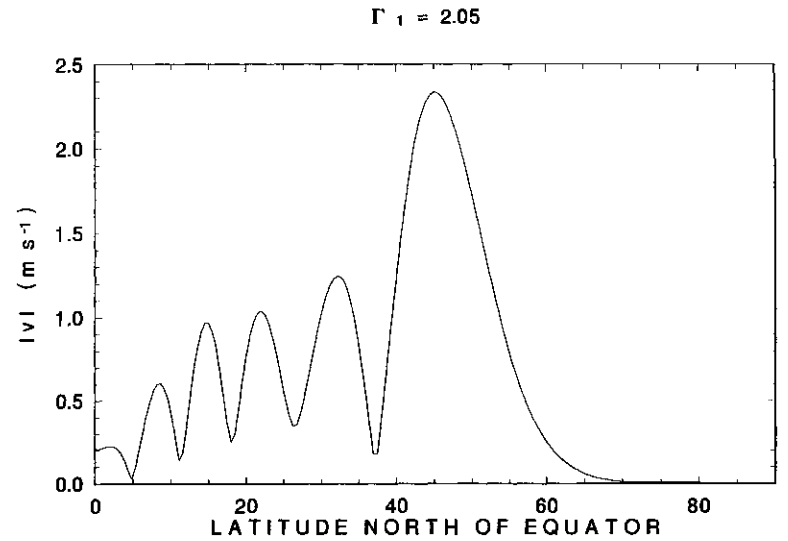

FIG. 9.—The latitudinal structure of the magnitude of the tidal zonal velocity at cloud level for an interior with $\Gamma_1 = 2.05$. The dominant response is concentrated at the 12th mode (viz. Fig. 2).

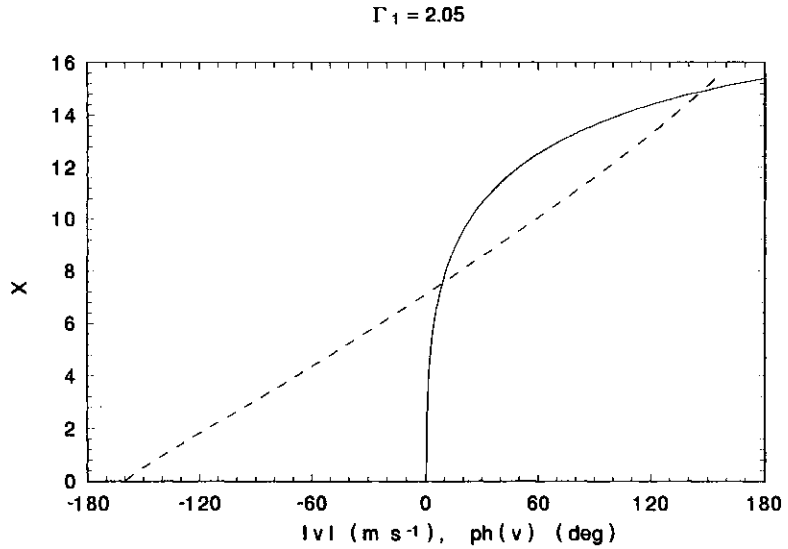

FIG. 10.—The vertical structure of the tidal zonal velocity at the equator as a function of height, measured in pressure scale heights. In the interior $\Gamma_1 = 2.05$. The reference level $X = 0$ corresponds to the tropopause. The solid curve is the magnitude, and the dashed curve is the phase in degrees. Breaking occurs at $X \approx 12$.

ence pressures and densities, and $\gamma = c_p/c_v$. Note that T^p_{oz} is related to the Brunt-Väisälä frequency by

$$T^p_{oz} = \frac{\gamma N^2}{g_s}, \tag{3.4}$$

where g_s is the gravitational acceleration at the surface of the planet. It may appear from equation (3.2) that the stream function is singular in regions of vanishing Brunt-Väisälä frequency, but as it will be shown shortly, this is not actually the case.

We define a residual meridional flow U^*, W^* by

$$\overline{\rho u} = U^* + \bar{\psi}_z, \tag{3.5a}$$

$$\overline{\rho w} = W^* - \frac{1}{a \sin\theta}\bar{\psi}_\theta, \tag{3.5b}$$

and transform equation (3.1) to

$$(\rho_0 \bar{v})_t + 2\omega \cos\theta U^* = -\frac{1}{a \sin^2\theta}(\rho_o \overline{uv} \sin^2\theta)_\theta - \left(\rho_o \overline{vw} + 2\omega \cos\theta \rho_o \frac{\overline{uT^p}}{T^p_{oz}}\right)_z. \tag{3.6}$$

The right-hand side of equation (3.6) has been written as a divergence of a flux vector, commonly called the Eliassen-Palm flux, with the property that it is divergenceless in the absence of dissipation, transience, or forcing (Andrews & McIntyre 1976; Boyd 1976). In such circumstances there is no modification of the mean flow by the tidal fields. In the presence of dissipation, transience and/or external forcing, the divergence of the Eliassen-Palm flux gives the acceleration of the mean zonal velocity caused by the tidal fields.

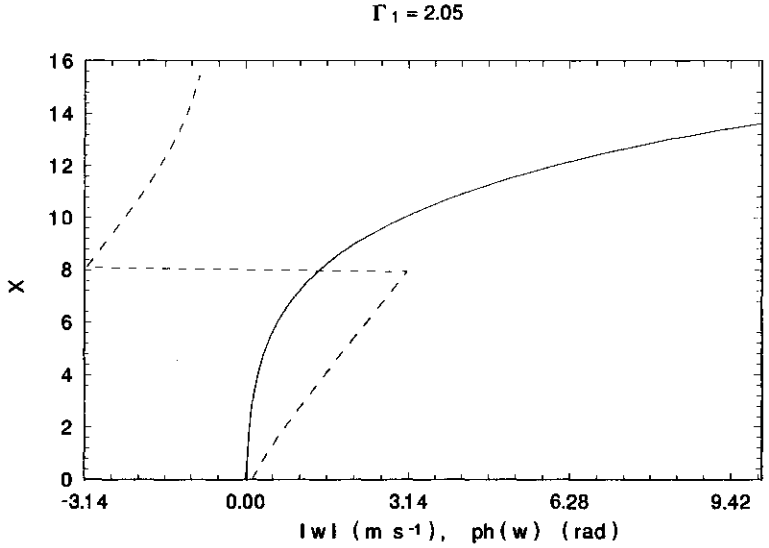

FIG. 11.—The vertical structure of the tidal vertical velocity at the equator as a function of height, measured in pressure scale heights. In the interior $\Gamma_1 = 2.05$. The reference level $X = 0$ corresponds to the tropopause. The solid curve is the magnitude, and the dashed curve is the phase in degrees. Breaking occurs at $X \approx 12$.

The radiative relaxation time at cloud level on Jupiter is estimated to be of the order of a Jovian year (Flasar 1989; Gierasch & Goody 1969). Disregarding diabatic heating, the first of law of thermodynamics takes the form:

$$T^p_t = -wT^p_{oz} . \tag{3.7}$$

Multiplying equation (3.7) by the southward displacement ζ (i.e., $\zeta_t = u$) and zonally averaging in the absence of transience we obtain

$$\overline{T^p u} = \overline{\zeta w} T^p_{oz} , \tag{3.8}$$

which shows that the streamfunction $\bar{\psi}$ is an indeterminate form with a finite limit as $T^p_{oz} - > 0$ (even with diabatic heating included, this procedure carries over as long as the diabatic heating vanishes at the neutral regions). Substituting equation (3.8) in equation (3.6) we get

$$(\rho_o \bar{v})_t + 2\omega \cos\theta U^* = -\frac{1}{a \sin^2\theta}(\rho_o \overline{uv} \sin^2\theta)_\theta + \frac{s}{a\sigma \sin\theta}(\rho_o \overline{wP})_z , \tag{3.9}$$

where $P = \Omega + p/\rho_o$ is the reduced pressure. To arrive at equation (3.9) we made use of the identity:

$$[\rho_o \overline{w(v + 2\omega \cos\theta\zeta)}]_z = -\frac{s}{a\sigma \sin\theta}(\rho_o \overline{wP})_z , \tag{3.10}$$

and assumed that the tidal fields vary harmonically as $e^{i(\sigma t + s\phi)}$, where ϕ is the azimuthal angle (the zonal wavenumber for gravitational tidal excitation is $s = 2$).

Typical maximum magnitudes of the E-P flux indicating the magnitude of the mean flow acceleration tendency as a function of the interior stability are shown in Figure 12. If we disregard the values of interior stratification that lead to especially amplified atmospheric response, the accelerations for a stratified interior are of the order of 1 cm s^{-1} d^{-1}. For those interior stratifications for which the response is amplified we may expect up to two orders of magnitude larger accelerations. A typical meridional structure of the acceleration tendency is shown in Figure 13. Note that the mean flow modifications are limited to a region equatorward of 50°, and provide a structured momentum source that could maintain multiple jets and bands qualitatively similar to those observed on Jupiter.

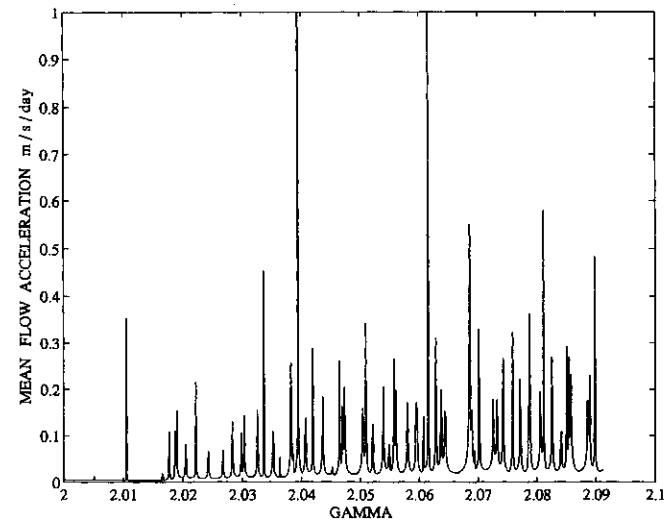

FIG. 12.—The magnitude of the equatorial acceleration tendency at cloud level in ms^{-1} d^{-1} as a function of the stability in the interior measured by Γ_1.

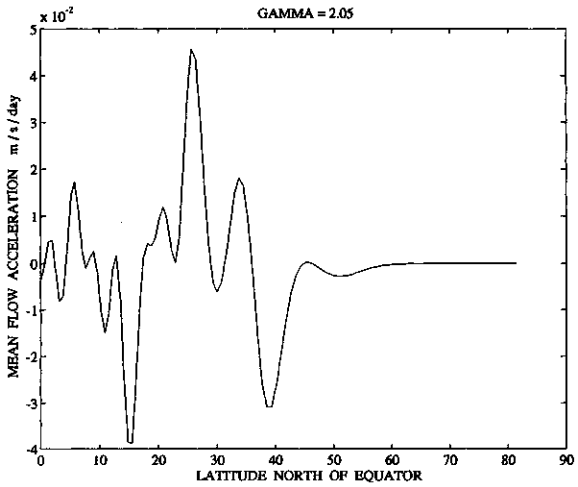

FIG. 13.—The latitudinal structure of the acceleration tendency of the mean zonal velocity at cloud level in ms^{-1} d^{-1} for an interior with $\Gamma_1 = 2.05$.

4. DISCUSSION

Despite the faint and latitudinally homogeneous solar and interior thermal forcing, the Jovian atmosphere assumes a banded structure with a multitude of zonal jets. The origin of this atmospheric phenomenon remains unexplained. Previous work sought an explanation for the latitudinal structure of the atmospheric circulation based on the effect of rotation on dynamics. Williams (1979) proposed that the observed circulation is a shallow atmospheric phenomenon: the manifestation of inherent zonal organization of rapidly rotating turbulent flows, observed to occur in computer simulations of turbulence on the surface of a rotating sphere. Busse (1976, 1983) proposed that the zonal jets are manifestation of deep flows associated with the cylindrically symmetric organization of convection in rapidly rotating planets.

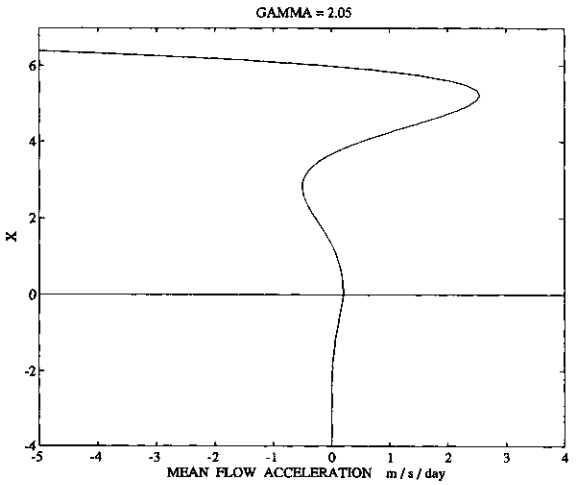

FIG. 14.—The vertical structure of the tidal acceleration tendency of the mean zonal velocity at cloud level in ms^{-1} d^{-1} at the equator as a function of height, measured in pressure scale heights. In the interior $\Gamma_1 = 2.05$. The reference level $X = 0$ corresponds to the tropopause.

An alternative mechanism for the maintenance of the banded structure proposed by Lindzen (1991) was investigated in this paper. According to this mechanism the gravitationally excited tides on Jupiter may maintain the meridionally varying zonal flows through their Eliassen-Palm flux divergences. A direct implication of this mechanism is the latitudinal concentration of the zonal flows equatorward of the critical latitude arising from the dominant tidal response. If the dominant tidal response is due to the satellite with the largest contribution to the tidal potential this theory predicts that the bands on Jupiter should be located equatorward of 50° (corresponding to the critical latitude of the forcing due to Io), on Saturn equatorward of 76° (due to the gravitational tidal forcing of Titan), and on Uranus equatorward of 46° (due to the gravitational tidal forcing of Ariel). The retrograde orbit of Triton around Neptune precludes the existence of a critical latitude, but the case of Neptune warrants separate treatment due to the highly inclined orbit of its satellite. It should be noted that given the potentially large variations in response, one cannot trivially dismiss the possibility that satellites with smaller tidal potentials can have significant effects. However, the dominance of the potential due to Io (and of Titan, Ariel, and Triton on Saturn, Uranus and Neptune) is so large (Lindzen 1991; ILa) that barring exceptional circumstances they may be presumed to dominate.

The analysis we have presented shows that for this mechanism to be viable the planet must be sufficiently stratified below the cloud cover. If there is no stratification, the tidal response is weak and is concentrated at the gravest meridional mode which does not possess the observed highly varying latitudinal structure. When there is stratification the response is dominated by a higher order Hough mode and the induced mean flow tendency assumes a structure that could induce banding. The magnitude of the induced tendency was found to be of the order of 1 cm s^{-1} d^{-1} or greater. The lack of observations of the eddy dissipation at cloud level precludes calculation of the magnitude of the induced zonal jets (however, there are indications that the appropriate dissipation time may be of the order of 2–4 months; Ingersoll 1990). The required stability in the interior is small ($N \approx 5$–$10\ \sigma$) and we expect that direct observations could not distinguish such a state from that of neutrality. Our calculations also indicate that the stable regions must be located at the outer parts of the planet (fractional radius >0.9) where the pressure scale heights are relatively small. The precise structure of the stability in these regions is unimportant provided that the response is governed by wave dynamics.

The proposed role for tides in maintaining the banded structure of Jupiter's atmosphere depends on the existence of interior stability. At this point the primary indication in support of a finite stability in the interior of the planet is the success of the theory in accounting for the tidal dissipation in Jupiter required by the orbital evolution of Io. The amplitudes calculated in this paper suggest that confirmation by direct observation of the tidal response at cloud level should also be possible.

We thank H. Houben for helpful comments. This work was supported by NASA Grant NAGW-525 and NSF Grant ATM-914441. P. J. Ioannou acknowledges the support of NSF ATM-9216189.

REFERENCES

Andrews, D. G., & McIntyre, M. E. 1976, J. Atm. Sci., 33, 2031
Boyd, J. 1976, J. Atm. Sci., 33, 2285
Busse, F. H. 1976, Icarus, 29, 255
———. 1983, Geophys. Astrophys. Fluid Dyn., 23, 153
Deming, D., Mumma, M. J., Espenak, F., Dennings, D. E., Kostiuk, Th., Wiedemann, G., Loewenstein, R., & Piscitelli, J. 1989, ApJ, 343, 456
Flasar, F. M. 1989, in Time Varying Phenomena in the Jovian System, ed. M. J. S. Belton, R. A. Weston, & J. Rahe (Washington, DC: NASA), 324
Gierasch, P. J., & Goody, R. 1969, J. Atm. Sci., 26, 979
Gill, A. E. 1982, Atmosphere-Ocean Dynamics (New York: Academic)
Hou, A. Y., & Farrell, B. F. 1987, J. Atm. Sci., 44, 1049
Houben, H. C. 1978, Ph.D. thesis, Cornell Univ.
Ingersoll, A. 1990, Science, 248, 308
Ioannou, P. J., & Lindzen, R. S. 1993a, ApJ, 406, 252 (ILa)
———. 1993b, ApJ, 406, 266 (ILb)
Lindal, G. F., et al. 1981, J. Geophys. Res., 86, 8721
Lindzen, R. S. 1981, J. Geophys. Res., 81, 9707
———. 1988, J. Atmos. Sci., 45, 705
———. 1991, Geophys. Astrophys. Fluid Dyn., 58, 123
Lindzen, R. S., & Hong, S.-S. 1974, J. Atm. Sci., 31, 1421
Williams, G. P. 1979, J. Atmos. Sci., 36, 932